Geometrical representation of sum frequency generation and adiabatic frequency conversion

Haim Suchowski,[1,*] Dan Oron,[1] Ady Arie,[2] and Yaron Silberberg[1]
[1]*Department of Physics of Complex System, Weizmann Institute of Science, Rehovot 76100, Israel*
[2]*School of Electrical Engineeing, Faculty of Engineering, Tel Aviv University, Tel Aviv, Israel*
(Received 1 May 2008; revised manuscript received 22 October 2008; published 15 December 2008)

We present a geometrical representation of the process of sum frequency generation in the undepleted pump approximation, in analogy with the known optical Bloch equations. We use this analogy to propose a technique for achieving both high efficiency and large bandwidth in sum frequency conversion using the adiabatic inversion scheme. The process is analogous with rapid adiabatic passage in NMR, and adiabatic constraints are derived in this context. This adiabatic frequency conversion scheme is realized experimentally using an aperiodically poled potassium titanyl phosphate (KTP) device, where we achieved high efficiency signal-to-idler conversion over a bandwidth of 140 nm.

DOI: 10.1103/PhysRevA.78.063821 PACS number(s): 42.65.Ky, 42.25.Fx, 42.70.Qs

The generation of tunable optical radiation typically relies on nonlinear frequency conversion in crystals. In this process, light of two frequencies is mixed in a nonlinear crystal, resulting in the generation of a third color at the sum or difference frequency. These three-wave mixing processes, also known as frequency upconversion or downconversion, are typically very sensitive to the incoming frequencies, due to the requirement of phase matching. Thus angle, temperature or other tuning mechanisms are needed to support efficient frequency conversion. This particularly affects efficient conversion of broadband optical signals, since simultaneous phase matching of a broad frequency range is hard to achieve.

Solving the general form of the wave equations governing three wave mixing processes in a nonlinear process is not an easy task. The three nonlinear coupled equations can be simplified assuming that one incoming wave (termed pump) is much stronger than the other two. This "undepleted pump" approximation results in two linear coupled equations rather than the three nonlinear ones [1]. In the case of the sum frequency generation (SFG) process, this simplified system possesses SU(2) symmetry, sharing its dynamical behavior with two other states systems, such as nuclear magnetic resonance (NMR) and the interaction of coherent light with a two-level atom [2]. In this paper we explore this analogy, and in particular the geometrical visualization using the approach presented by Bloch [3] and Feynman *et al.* [4]. The simple vector form of the coupling equation can bring physical insight into the problem of frequency conversion, enabling a more intuitive understanding of the effects of spatially varying coupling and phase mismatch. The utility of this approach is demonstrated by introducing a robust, highly efficient method for broadband wavelength conversion based on the mechanism known as rapid adiabatic passage (RAP) [5]. The demonstration is experimentally realized using an adiabatically varying aperiodically poled potassium titanyl phosphate (APPKTP) in a quasiphased matched (QPM) design.

Aperiodically poled structures have already been introduced for improving the bandwidth response of frequency conversion, but at a cost of a significantly reduced efficiency [6–8]. The broad bandwidth response is in particular important for frequency conversion of ultrashort pulses. Chirped QPM gratings have been utilized to manipulate short pulses both in second harmonic generation (SHG) [9–11], difference frequency generation (DFG) [12], and in parametric amplification [10,13]. Recently, crystals with random QPM was shown to exhibit extremely broad bandwidth, although at a price of severe reduction of the conversion efficiency [14]. While in standard frequency conversion processes, the crystal parameters and the pump intensity should be precisely controlled in order to reach high conversion efficiency, we show that by utilizing adiabatic frequency conversion one can still reach nearly 100% conversion efficiency over a broad wavelength and temperature range. In our demonstration we succeed in achieving near complete conversion while maintaining extremely broad bandwidth of over 140 nm.

Let us first consider the geometrical representation of SFG. In the undepleted pump approximation, the pump amplitude is assumed constant along the nonlinear crystal, and the following normalized coupled equations can be constructed [1]:

$$i\frac{d\tilde{A}_1}{dz} = \kappa \tilde{A}_3 e^{-i\Delta k z}, \tag{1a}$$

$$i\frac{d\tilde{A}_3}{dz} = \kappa^* \tilde{A}_1 e^{+i\Delta k z}. \tag{1b}$$

Here, $\Delta k = k_1 + k_2 - k_3$ is the phase mismatch, z is the position along the propagation axis, $\kappa = \frac{4\pi w_1 w_3}{\sqrt{k_1 k_3} c^2}\chi^{(2)} A_2$ is the coupling coefficient. The normalized signal and idler amplitudes are $\tilde{A}_1 = \frac{c}{4\omega_1}\sqrt{\frac{k_1}{\pi\chi^{(2)} A_2^*}} A_1$ and $\tilde{A}_3 = \frac{c}{4\omega_3}\sqrt{\frac{k_3}{\pi\chi^{(2)} A_2}} A_3$, where ω_1 and ω_3 are the frequencies of the signal and idler, respectively, k_1 and k_3 are their associated wave numbers, c is the speed of light in vacuum, A_1, A_2, A_3 are the signal, pump, and idler amplitudes, respectively, and $\chi^{(2)}$ is the second order susceptibility of the crystal. Without loss of generality, we choose such that $\omega_1 + \omega_2 = \omega_3$.

These coupled wave equations have the same form as those describing the dynamics of quantum mechanical two

*Haim.suchowski@weizmann.ac.il

TABLE I. Analogy between the SFG process in the undepleted pump approximation and the dynamics of a two level atomic system, induced by coherent light. The middle column describes the optical Bloch sphere realization of the two level systems (Ref. [2]). The right column shows the analogous parameters of the SFG sphere realization.

Parameter	Optical Bloch sphere	SFG sphere realization
Evolution parameter	time	z axis
Ground/excited state population	$\lvert a_g\rvert^2, \lvert a_e\rvert^2$	$\lvert A_1\rvert^2, \lvert A_3\rvert^2$
Energy difference	$\omega_0=\omega_{fg}$	$n(\omega_2)\omega_2/c$
Detuning/phase mismatch	Δ	Δk
"Rabi" frequency	$\Omega_0=\frac{1}{\hbar}\mu E_{in}$	$\kappa=\frac{4\pi w_1 w_3}{(k_1 k_3)^{1/2}c^2}\chi^{(2)}E_2$
Torque vector	$\Omega=(\mathrm{Re}\{\Omega_0\},\mathrm{Im}\{\Omega_0\},\Delta)$	$g=(\mathrm{Re}\{\kappa\},\mathrm{Im}\{\kappa\},\Delta k)$
State vector—ρ	$(\mathrm{Re}\{a_f^* a_g\},\mathrm{Im}\{a_f^* a_g\},\lvert a_f\rvert^2-\lvert a_g\rvert^2)$	$(\mathrm{Re}\{A_3^* A_1\},\mathrm{Im}\{A_3^* A_1\},\lvert A_3\rvert^2-\lvert A_1\rvert^2)$

level systems. Their dynamics is dictated by $\Delta k(z)$ and κ, and can be solved analytically only for limited cases. One such solvable example is when the phase mismatch is constant [1]. In this case, full energy transfer from signal to idler (A_1 to A_3 conversion, which is termed as SFG or upconversion process) is achievable *only* in the case of perfect phase matching along the entire propagation, i.e.,$\Delta k(z)=0$, and only when $\kappa\cdot z=n\pi$ is satisfied with odd n. Other constant phase mismatch results in an inefficient frequency conversion. Methods for approximate solutions, such as perturbation theory, are also available. In the weak coupling limit, the dynamics can be solved fully in the Fourier domain [12], but due to its perturbative nature, it will be limited to low conversion values. In general, this complex valued dynamics, which posses SU(2) dynamical symmetry, and in particular when the phase mismatch parameter varies along the propagation, there is no known analytical solution, a statement which is also true in NMR and in light-matter interaction two level problems [2,15]. A recent review summarizes the known analytical solutions in the context of coherent light interaction with two level systems [15]. For those cases which are not solvable analytically, it is convenient to use the geometrical representation, with which one gains a physical intuition on the conversion along the propagation, without solving or simulating the process.

We adopt Feynman *et al.* [4] formulation and write the dynamics of this problem as a real three dimensional vector equation, which can be visualized geometrically on a sphere, known as the Bloch sphere. In this context, we define a state vector, $\vec{\rho}_{SFG}=(U,V,W)$ as follows:

$$U_{SFG}=A_3^* A_1+A_1^* A_3, \tag{2a}$$

$$V_{SFG}=i(A_3^* A_1-A_1^* A_3), \tag{2b}$$

$$W_{SFG}=\lvert A_3\rvert^2-\lvert A_1\rvert^2. \tag{2c}$$

This vector represents the relation between the signal and idler fields along the crystal. In particular, the z component (W_{SFG}) gives information about the conversion efficiency. The south pole $\vec{\rho}=(0,0,-1)$ corresponds to zero conversion ($A_3=0$), while the north pole $\vec{\rho}=(0,0,1)$ corresponds to full conversion. In between, the conversion efficiency can be evaluated by $\eta=(W_{SFG}+1)/2$. The torque vector $\vec{g}=(\mathrm{Re}\{\kappa\},\mathrm{Im}\{\kappa\},\Delta k)$ represents the coupling between the two fields. The loss-free evolution equations can be written as a single vector precession equation:

$$\frac{d\vec{\rho}_{SFG}}{dz}=\vec{g}\times\vec{\rho}_{SFG}. \tag{3}$$

There is a clear analogy then between the two-level system and frequency conversion: The population of the ground and excited states are analogous to the magnitude of the signal (A_1) and idler (A_3) fields, respectively. Time evolution is replaced by propagation along the z axis, and the detuning Δ is replaced by the phase-mismatch Δk value; this analogy is further detailed in Table I. In this context, a perfect phased matched solution for full conversion [1] has the same dynamical trajectory on the Bloch sphere surface as on-resonant interaction in atomic physics [2]. This results in oscillatory dynamics between the two modes ("Rabi oscillations"). An odd π pulse in optical resonance is analogous to full transfer of energy from ω_1 to ω_3, which is known as an upconversion process. This can be visualized in the Bloch sphere representation as a rotation of the SFG state vector from the south pole to the north pole. Any phase mismatch leads to a dynamics similar to a detuned resonance interaction, which exhibits faster oscillations and lower conversion efficiencies, as shown in Fig. 1(c). Note that due to the symmetry of the coupled equations, one can start the process with ω_3 as input frequency (assuming $\omega_3>\omega_2$). In this case $A_1(z=0)=0$, and a difference frequency generation (DFG) process between the weak input at ω_3 and the strong pump (ω_2) will occur, resulting in generation of the lower frequency ($\omega_1=\omega_3-\omega_2$). The equivalent Bloch sphere representation is a rotation of the state vector from the north pole toward the south pole.

This analogy could be extended to include the semiphenomenological decay constants T_1 and T_2, which appear in the original Bloch equations. In nuclear resonance, those are called the longitudinal and the transverse lifetimes (for spins they govern the decay of the magnetic spin components

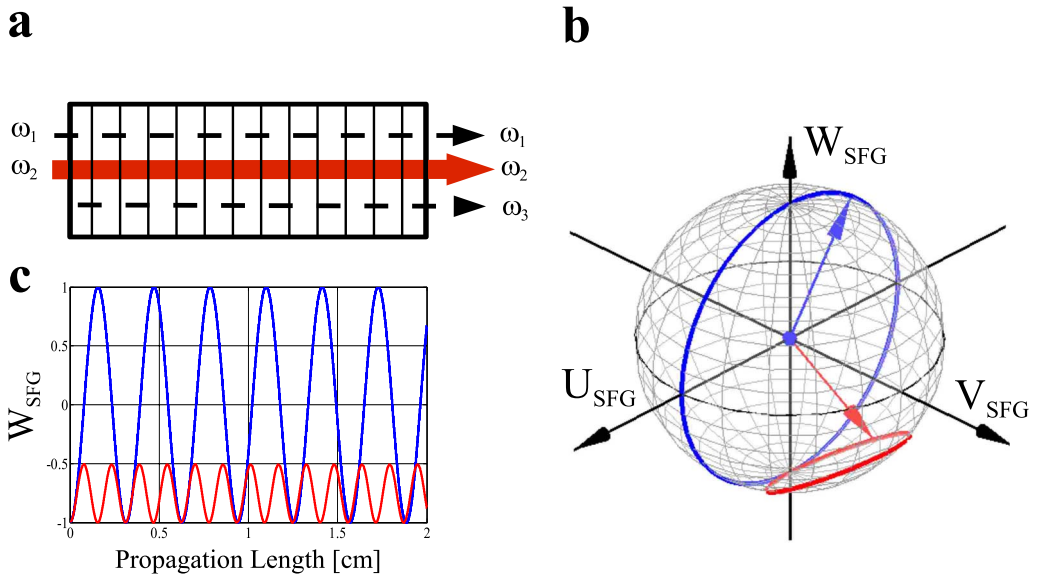

FIG. 1. (Color online) Bloch sphere geometrical representation of SFG in the undepeleted pump approximation. (a) A periodically poled quasiphased crystal with a constant phase matching value along the propagation. (b) Geometrical visualization of the SFG dynamics on a SFG Bloch sphere. Two trajectories are plotted: perfect phase matching (blue, torque vector points to the equator) which can result in efficient conversion and a constant nonzero phase mismatch (red, torque vector points to a point in the south hemisphere), *always* resulting in an inefficient conversion process. (c) The projection of the trajectory onto the z axis yields the conversion efficiency.

which are parallel or perpendicular static components of the magnetic field). In our context, these parameters are characteristics length scales rather than times. The $1/T_1$ relaxation coefficient is related to the characteristic absorption (or loss) length along the propagation $[\alpha(\omega_i)]$. Loss results in the decrease of the total intensity of the process along the propagation direction, i.e., $|A_1(z)|^2+|A_3(z)|^2<|A_1(0)|^2+|A_3(0)|^2$, and is visualized in the Bloch sphere representation, as the shrinking of the state vector toward the origin. The $1/T_2$ relaxation parameter, which is related to the decay of polarization through dephasing and loss, could be included to describe random distribution of wave vectors, pointing slightly different from the propagation axis, effecting dramatically on the phase mismatch parameter and thus conversion efficiency. In order not to obscure the main features of the analogy, and due to the fact that the typical values of loss in such processes for the near IR and visible regimes in standard crystals are less than $1\%/\mathrm{cm}$, we decided not to include these parameters in the current model. We note that they could add new insight to the dynamics of this SFG process in the presence of loss and dephasing, which might be important near crystal resonances (in the near UV for KTP), where losses become non-negligible.

Due to the above, achievement of full energy transfer in an upconversion process is usually not robust, requiring several ingredients to be simultaneously satisfied. However, from the above analogy we can adopt the RAP mechanism [5], where a strong chirped excitation pulse scans slowly through resonance to achieve robust full inversion, to the realm of frequency conversion. Thus in order to transfer from $A_1(z)$ to $A_3(z)$ the phase mismatch parameter, $\Delta k(z)$ should be very large compared to κ, and has to change adiabatically from a big negative (positive) value to a large positive (negative) value along the crystal. The adiabaticity condition requires that

$$\left|\frac{d\Delta k}{dz}\right| \ll \frac{(\Delta k^2+\kappa^2)^{3/2}}{\kappa}. \tag{4}$$

If the rate of variation is not slow enough, or the coupling coefficient is not large enough, this inequality would not be satisfied and the conversion efficiency will be poor. Figure 2 demonstrates the case when all those constraints are satisfied and full frequency conversion is achieved.

This picture could also hold for efficient upconvertion of ultrashort pulses. For this to happen, the dispersion properties of the nonlinear crystal, which have an impact on the temporal envelope, have to be considered. Note, first, that the pump wave, which remains always a narrow band along the propagation, does not put any limitation from the dispersion point of view. Second, in the adiabatic limit, the conversion process occurs in a localized region along the crystal, as illustrated in Fig. 2(c). An estimation of this characteristic length [16] is $L_{eff}=\frac{\kappa}{d\Delta k/dz}$. The main effects that should be considered in this context are group velocity mismatch (GVM), and group velocity dispersion (GVD). GVM causes a temporal walkoff of the incoming signal pulse (ω_1) and the generated idler pulse (ω_3) due to their different group velocities. A second order process due to GVD leads to an addition of linear chirp along the propagation. For both effects to be negligible, their characteristic lengths should be much larger than the adiabatic effective length mentioned above. A standard estimation of the effect of GVM on short pulse propagation is $L_{GVM}=\frac{\tau}{GVM}$, with $GVM=(\frac{1}{u_g(\lambda_1)}-\frac{1}{u_g(\lambda_3)})$, and $u_g(\lambda_i)$ is the group velocity of wavelength λ_i. In order to minimize GVM, one should ask for overlapping of the signal (ω_1) and idler (ω_3) pulses along the conversion length, i.e., $L_{eff} \ll L_{GVM}$. The minimal temporal width of the pulse should therefore be $\tau_{GVM}=L_{eff}$ GVM. For near IR to visible conversion, this translates to about 1 ps. However, this does not

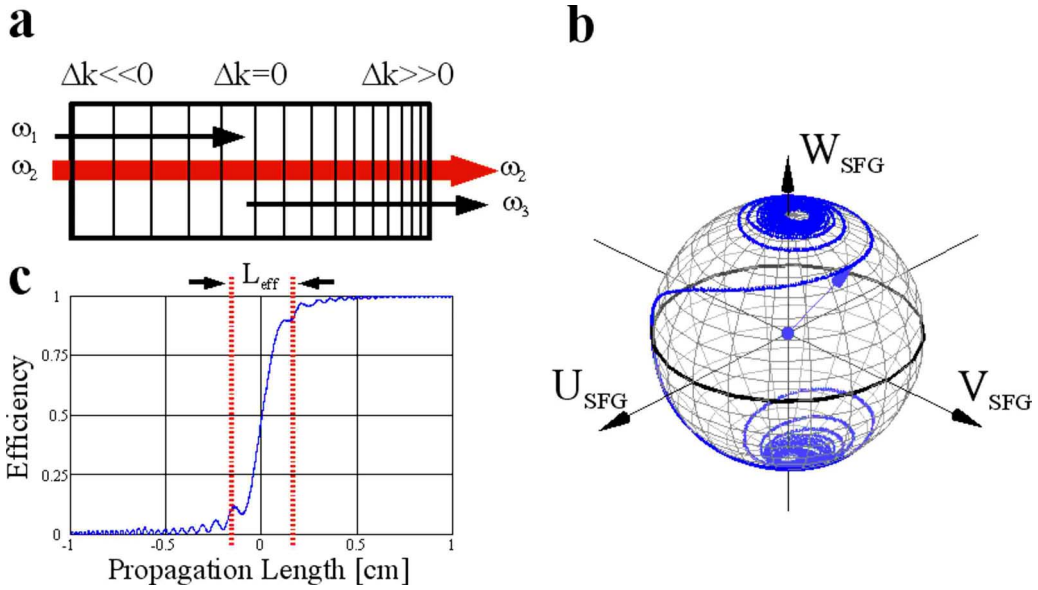

FIG. 2. (Color online) Adiabatic conversion scheme of SFG. (a) Continuous adiabatic variation of the phase mismatch parameter is required. (b) The adiabatic following trajectory, where the torque vector initially points to the vicinity of the south pole, and ends up at the vicinity of the north pole. (c) The projection of the trajectory onto the z axis. In this trajectory, a phase matching condition is fulfilled only at $z=1$ cm, and the effective length of the conversion is 3 mm (dashed red line).

mean that shorter pulses cannot be converted: in order to convert a transform limited 100 fs pulse, one should prestretch the pulse to approximately 10 ps by adding linear chirp. This chirp, which reduces the effect of temporal walkoff, should be removed at the output of nonlinear crystal. This described mechanism is analogous to the chirped pulse amplification method [17]. The second order effect of GVD is defined by $\beta=\frac{d^2w}{dk^2}$, and its characteristic length is $L_{GVD}=\frac{\tau^2}{\beta}$. The GVD parameter which should be used in this calculation is this of the shorter wavelength, which is typically the larger one. In our design L_{GVD} ($\lambda=620$ nm) ≈ 2.5 cm. This value satisfies $L_{eff} \ll L_{GVD}$, and thus can be neglected. We checked that higher order dispersion effects can be neglected as well. Another inherent phenomenon which exists in wavelength conversion through aperiodically poled structures is the addition of linear chirp, positive or negative, when propagating along the crystal [9–12]. This chirp, too, can be removed at the output.

In the experimental realization of this adiabatic conversion scheme we utilize the technique of QPM [18]. By tuning the spatial structure of the domains, this technique allows us to design almost any desired function of the phase mismatched parameter. In particular, it is possible to achieve an effective phase mismatch parameter which is the summation of the process phase mismatch and the artificial phase mismatch, i.e., $\Delta k_{eff}(z)=k_{signal}+k_{pump}-k_{idler}-\Delta k_{\Lambda}(z)$. The desired phase-mismatch parameter is achieved by poling the QPM structure using the approximate relation: $\Delta k_{\Lambda}(z)=\frac{2\pi}{\Lambda(z)}$, where $\Lambda(z)$ is the local poling period.

An adiabatic APPKTP was designed to satisfy the constraints posed by Eq. (4). The periodicity was varied from 14.6 to 16.2 μm along a crystal length of $L=17$ mm, to induce a linear adiabatic is required for adiabatic full conversion, change in $k_{eff}(z)$. An intensity of 90 MW/cm^2 is required for full adiabatic conversion, much lower value than the damage threshold of KTP crystal which is approximately 500 MW/cm^2 [19]. The design was carried out by a numerical simulation of the process propagation of Eq. (1) using the finite difference method. We used an optical parametric oscillator system (Ekspla NT342) to produce simultaneously a strong pump at 1064 nm (6 ns, 130 μJ), and a tunable signal that could be varied from 1400 to 1700 nm (5 ns, 1 μJ). The pump and the signal, both polarized in the extraordinary axis, were spatially overlapped and focused collinearly into the crystal with waists of 150 and 120 μm^2, respectively. These values guarantee that the Rayleigh range is larger than the crystal length. We recorded the input signal and the output SFG signal by an InGaAs detector and a cooled charge-coupled device (CCD) spectrometer, respectively.

We first examined the dependence of the conversion efficiency on the pump intensity at fixed signal wavelength of 1530 nm. The conversion efficiency was measured by comparing the signal intensity with and without the presence of the pump. This was checked to be completely correlated with the observed SFG intensity and free of thermal effects. The results are presented in the inset of Fig. 3; good correspondence is obtained with numerical simulation. We also measure the conversion efficiency as a function of signal wavelength at a constant pump intensity of 15 MW/cm^2 and at room temperature. We show in Fig. 3 efficient broadband conversion of over 140 nm wide (1470–1610 nm). This is in good correspondence with the numerical simulation of the design (dashed-dotted blue line), except for a small region of low efficiency around 1485 nm, which is associated with a manufacturing defect, thus causing the violation of the adiabaticity condition. Note that a standard periodically poled structure designed to achieve perfect phase matching would lead to efficient broadband conversion over a 2-nm bandwidth only.

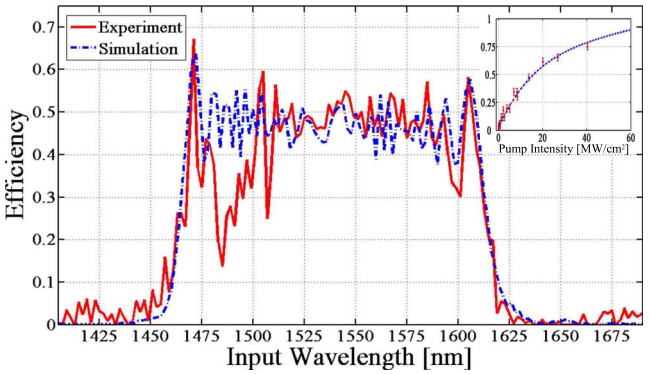

FIG. 3. (Color online) Conversion efficiency as a function of input wavelength using the adiabatic APPKTP design at a pump intensity of 15 MW/cm^2 at room temperature. Inset: Conversion efficiency as a function of pump intensity with an input wavelength of 1530 nm. The maximal conversion efficiency was $74\% \pm 3\%$.

The adiabatic conversion scheme is robust to variations in the parameters of the crystal as well as of the light. In particular, the conversion efficiency is insensitive to input wavelength, crystal temperature, pump intensity, crystal length, and the angle of incidence. A detailed study of the properties of this particular converter will be presented in a forthcoming publication.

In conclusion, we show that a geometrical Bloch sphere visualization can be used to describe the evolution of the complex mode amplitudes in a SFG process. We use this picture to design a high efficiency wavelength converter which is the analog of adiabatic rapid passage in two level systems. It is important to note that the quasiphase matched crystal is only one possible realization; the same mechanism can be applied, for example, by inducing a temperature gradient on a perfect phased matched crystal, or by any other mechanism fulfilling the adiabatic constraints. The present scheme can be utilized for efficient frequency conversion of broadband signals as well as ultrashort pulses. It will be valid only if the ultrashort pulse will initially stretch, then upconverted, and finally recompressed at the output. This analysis holds promise for efficient upconversion of braodband fluorescent signals as well as ultrashort pulses in a wide range of frequencies from UV to far IR. It may be particularly useful in the efficient upconversion of weak infrared signals to the near-infrared or visible range, used in atmospherical observation [20,21]. The generalization of this analogy to higher order nonlinear processes interaction can be made as well, and other known schemes from atom-photon interaction or NMR, such as stimulated Raman adiabatic passage (STIRAP) [22,23] can be adopted.

This research was supported by ISF (Grants No. 1621/07 and No. 960/05). H.S. is grateful to the Azrieli Foundation for financial support.

[1] R. W. Boyd, *Nonlinear Optics* (Academic, New York, 2003).
[2] L. D. Allen and J. H. Eberly, *Optical Resonance and Two Level Atoms* (Wiley, New York, 1975).
[3] F. Bloch, Phys. Rev. **70**, 460 (1946).
[4] R. Feynman, F. Venon, and R. Hellwarth, J. Appl. Phys. **28**, 49 (1957).
[5] A. Massiah, *Quantum Mechanics* (North Holland, Amsterdam, 1962), Vol. II.
[6] M. L. Bortz, M. Fujimura, and M. Fejer, Electron. Lett. **30**, 34 (1994).
[7] K. Mizuuchi, K. Yamamoto, M. Kato, and H. Sato, IEEE J. Quantum Electron. **30**, 1596 (1994).
[8] H. Guo, S. H. Tang, Y. Qin, and Y. Y. Zhu, Phys. Rev. E **71**, 066615 (2005).
[9] M. A. Arbore, A. Galvanauskas, D. Harter, M. H. Chou, and M. M. Fejer, Opt. Lett. **22**, 1341 (1997).
[10] G. Imeshev, M. Arbore, M. Fejer, A. Galvanauskas, M. Fermann, and D. Harter, J. Opt. Soc. Am. B **17**, 304 (2000).
[11] D. S. Hum and M. M. Fejer, C. R. Phys. **8**, 180 (2007).
[12] G. Imeshev, M. Fejer, A. Galvanauskas, and D. Harter, J. Opt. Soc. Am. B **18**, 534 (2001).
[13] M. Charbonneau-Lefort, B. Afeyan, and M. M. Fejer, J. Opt. Soc. Am. B **25**, 463 (2008).
[14] M. Baudrier-Raybaut, R. Haidar, P. Kupecek, P. Lemasson, and E. Rosencher, Nature (London) **432**, 374 (2004).
[15] B. T. Torosov and N. V. Vitanov, J. Phys. A **41**, 155309 (2008).
[16] K. Mullen, E. Ben-Jacob, Y. Gefen, and Z. Schuss, Phys. Rev. Lett. **62**, 2543 (1989).
[17] D. Strickland and G. Mourou, Opt. Commun. **56**, 219 (1985).
[18] J. Armstrong, N. Bloembergen, J. Ducuing, and P. Pershan, Phys. Rev. **127**, 1918 (1962).
[19] D. N. Nikogosyan, *Nonlinar Optical Crystals* (Springer, New York, 2005).
[20] S. Brustlein, L. Del Rio, A. Tonello, L. Delage, F. Reynaud, H. Herrmann, and W. Sohler, Phys. Rev. Lett. **100**, 153903 (2008).
[21] R. W. Boyd, Opt. Eng. (Bellingham) **16**, 563 (1977).
[22] N. V. Vitanov, T. Halfmann, B. W. Shore, and K. Bergmann, Annu. Rev. Phys. Chem. **52**, 763 (2001).
[23] S. Longhi, Opt. Lett. **32**, 1791 (2007).